Journal of Hazardous Materials 171 (2009) 588–593

Contents lists available at ScienceDirect

Journal of Hazardous Materials

journal homepage: www.elsevier.com/locate/jhazmat

Adsorption of low concentration phosphine in yellow phosphorus off-gas by impregnated activated carbon

Xueqian Wang*, Ping Ning, Yan Shi, Ming Jiang

Faculty of Environmental Science and Engineering, Kunming University of Science and Technology, Kunming 650093, PR China

ARTICLE INFO

Article history:
Received 4 February 2009
Received in revised form 9 June 2009
Accepted 9 June 2009
Available online 18 June 2009

Keywords:
Activated carbon
Adsorption
PH_3

ABSTRACT

In order to utilize high concentration CO comprehensively, impregnated activated carbon sorbent and the catalytic oxidation reaction for PH_3 were investigated in this study. Carbon was impregnated with HCl, KNO_3, or hexanediol. The activated carbon modified by 7% (mass fraction) HCl could enhance the adsorption purification ability significantly. Raising the reaction temperature or increasing the oxygen content of the gas can improve the purification efficiency. The structure of the materials after modification was determined using nitrogen adsorption. The modification decreased the volume of pores smaller than 2 nm in diameter with the most noticeable change occurring in the micropores ranging from 0.3 nm to 1.5 nm in diameter. Decreases in micropore volume accounted for 87% of the total pore volume change. After the adsorption, the surface areas decreased 28%, 29% of which was due to decreased micropore surface. HCl significantly increased the performance of carbon as a PH_3 adsorbent when HCl impregnation was applied whereas the effects of other materials used in this study were much less pronounced. HCl present in the small pores probably acted as a catalyst for oxygen activation that caused PH_3 oxidation. As a result of this process, H_3PO_4 and P_4O_{10} were formed, strongly adsorbed, and present in the small pores ranging from 0.3 nm to 1.5 nm. In conclusion, this study provides evidence that CO from industrial off-gas can be purified and used as the raw material for a broader range of products.

1. Introduction

CO is present in a large portion of off-gas of yellow phosphorus, off-gas of airtight calcium carbide furnace, synthetic ammonia gas, and other industrial emissions that are very useful C1 (one carbon) chemical industry. However, the phosphorus, sulfur, fluorin, arsenic, and other impurities in off-gas cause synthesis catalyst poisoning [1]. Therefore, purification becomes a bottleneck limiting the application of high concentration CO as the raw material gas to produce methanoic acid, acetic acid, carbinol, and other high value products. For example, the off-gas of yellow phosphorus is an industrial exhaust produced from the production process. During yellow phosphorus production by use of an electric stove, there are 2500–3000 m^3 off-gas by-products in 1 ton of yellow phosphorus, in which the CO content is up to 80–95%. Only 20–25% off-gas of yellow phosphorus is used as the primary fuel (the heat value is 10,000 kJ/m^3) due to the existence of PH_3, H_2S, and HF. The rest of the off-gas has to be burnt and released. This practice not only pollutes the environment [2] but also wastes CO resources.

With the development of chemical technology, especially the advancement in carbonylation synthesis of CO [3], CO as a chemical raw material gas can be used to synthesize carbinol, methyl formate, ethylic acid, and other chemical products. If the industrial off-gas that contains almost 90% CO is used to synthesize C1 chemical products, dimethyl ether and other organic compounds with economic values may be synthesized by CO carbonylation, which will not only limit environmental pollution but also reduce the production cost. A precious resource like the off-gas of yellow phosphorus that contains rich CO has been used to produce products with only low added values such as sodium tripolyphosphate and the sodium metaphosphate. So far, most of the off-gas of yellow phosphorus is burnt and released due to the limiting factor that the off-gas contains impurities that can affect carbonylation synthesis. The problem of cleaning the off-gas has not been solved, especially regarding how the removal of phosphorus may directly affect the catalysts synthesized by carbonylation of CO [4]. The difficulty of the research is in removing PH_3 within the gas under the condition of low temperature and low oxygen content [5].

This research harnessed impregnation to produce adsorbents of PH_3-activated carbon mainly by testing the effects of the experimental conditions such as the types of activated carbon and impregnant, reacting temperature, and oxygen content on the adsorption purification of PH_3. This work also examined changes in

* Corresponding author. Tel.: +86 13888183303; fax: +86 871 5188981.
E-mail address: wxqian3000@yahoo.com.cn (X. Wang).

0304-3894/$ – see front matter © 2009 Elsevier B.V. All rights reserved.
doi:10.1016/j.jhazmat.2009.06.046

Table 1
Parameters of the different adsorbents.

Supports	Raw material	Granular shape and size (mm)	Mechanical strength (%)	S_{BET}[a] ($m^2\ g^{-1}$)	V_Σ[b] ($cm^3\ g^{-1}$)
ZSM	Molecular sieve	Spherical, 2 mm	95	600	0.2822
AC					
WZ-1	Coal-based activated carbon	Cylindrical, 2 mm	85	710	0.3231
WZ-2	Coal-based activated carbon	Cylindrical, 2 mm	85	761	0.3321
WZ-3	Coal-based activated carbon	Cylindrical, 2 mm	90	1188	0.5676

[a] Surface area determined by nitrogen adsorption at 77 K.
[b] Total pore volume.

the micro-mechanism of produced adsorbent surface by measuring specific surface area and pore structure and analyzing thermo-gravimeter and heat athermalization in the process of removing PH_3.

2. Materials and methods

2.1. Experimental materials

Activated carbon and zeolite (ZMS-5A) were used as supports in this study. The activated carbon WZ-3 was a commercial product with a particle size of 2.0 mm. WZ-3 was obtained from coal-based activated carbon (Chang Ge Qian Yuan Chemical Factory, Henan, China). ZSM (99.99%, Nankai University catalyst Co., Ltd., Tianjin, China), WZ-1 (99.99%, Jiulong Fine Chemical Factory, Chongqing, China), and WZ-2 (Chuanjiang Chemical Reagent Factory, Chongqing, China) were used in the experiments as references. Details of these supports used in this study are given in Table 1.

The supports (10 g ± 0.1 g) were washed 3 times by 150 mL of distilled water at 70 °C to remove soluble impurities on supports. The activated carbon (WZ-3) was impregnated with HCl, KNO_3, or hexanediol (wt% = 7%, 50 mL) at 20 °C and the solution was stirred for 24 h. After that, the solution was filtrated and the adsorbents were dried for 12 h at 110 °C. The samples were marked as HClW (HCl-impregnated activated carbon), KNO_3W (KNO_3-impregnated activated carbon), and HW (hexanediol-impregnated activated carbon).

2.2. Instrumentations

The dynamic volumetric method was used in the experiment. A cylinder containing a mixture of PH_3 and nitrogen in required concentrations were mixed in the mixer evenly with micro-air and introduced into the adsorption bed unit under the speed of 0.3–0.5 L/min. This adsorption reaction occurred in a stainless steel columnar reactor. Fig. 1 displays the schematic diagram of the experiment.

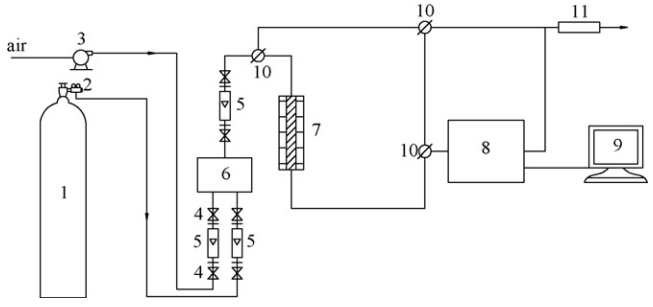

Fig. 1. Schematic diagram of the experiment. (1) Cylinder with PH_3; (2) Gas pressure reducer; (3) Vacuum pump; (4) Stop valve; (5) Flow meter; (6) Mixer; (7) Reactor for PH_3 with thermostatic apparatus; (8) Gas chromatography; (9) Chromatographic work station; (10) Three-way valves; (11) Collector.

2.3. Determination of PH_3

PH_3 was determined by gas chromatography–flame photometry under the following parameters: the flow rate of N_2 at 40 mL/min; column temperature at 50 °C, detector temperature at 200 °C, detection limit of 0.01 mg/m^3. The model of the gas chromatography was GC-14C (with flame photometric detector) with a polytetrafluoroethylene-packed column (GD-401 support).

2.4. Adsorption capacity of PH_3

The gas, containing 1100 mg/m^3 PH_3, under the flow rate of 0.3 L/min, went through the cylindrical absorbent layer that had a diameter of 9 mm and a height of 60 mm. The experiment was carried at temperatures between 20 °C and 110 °C. PH_3 was determined by off-gas chromatography. The experiment was stopped when the absorbent was saturated. After the experiment was ended, the adsorption capacity of PH_3, depending on the quality of the sorbent, was calculated with the corresponding integral according to formula (1) under various conditions of the breakthrough curves [6].

$$X = \frac{Qc_0t - Q\int_0^t c\,dt}{m} \quad (1)$$

In this formula: X = adsorption capacity, g/g; Q = gas flow, m^3/min; t = adsorption time, min; c_0 = adsorption column entrance mass concentration, mg/m^3; c = adsorption column outlet mass concentration, mg/m^3; m = adsorbent quality, g.

2.5. Nitrogen adsorption isotherms

Multi-spot nitrogen adsorption meter NOVA2000e (Quantachrome Corp) was used to determine nitrogen adsorption isotherms under 77.350 K. Adsorption isotherms were used to accurately calculate specific surface area, volume of micropores, total volume of pores, and micropore size distribution.

2.6. XPS measurements

Photoelectron spectra were obtained using X-ray photoelectron spectroscopy (XPS) analyses, which were carried out using a Physical Electronics PHI 5600 spectrometer. The X-ray source was operated by an Al Kα anode with a photo energy of hv 1486.6 eV. The core level binding energy of C1s for carbon at 284.8 eV was used as an internal reference for calibration.

2.7. Analyses of thermo-gravimetry and heat athermalization

Thermo-gravimetry and heat athermalization analyzer DTG-60H was used to analyze thermo-gravimetry and heat athermalization. The instrument parameters were as following: heating rate of 10 K/min, nitrogen flow rate of 100 mL/min.

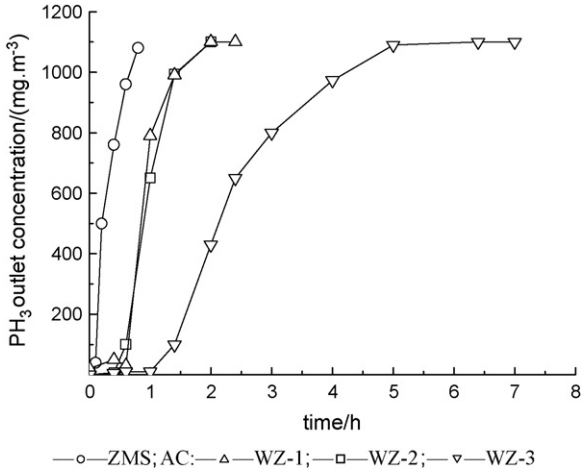

Fig. 2. Breakthrough curves of PH_3 on different adsorbents at 20 °C and 0.5% O_2 (PH_3 inlet concentration 1100 mg/m^3).

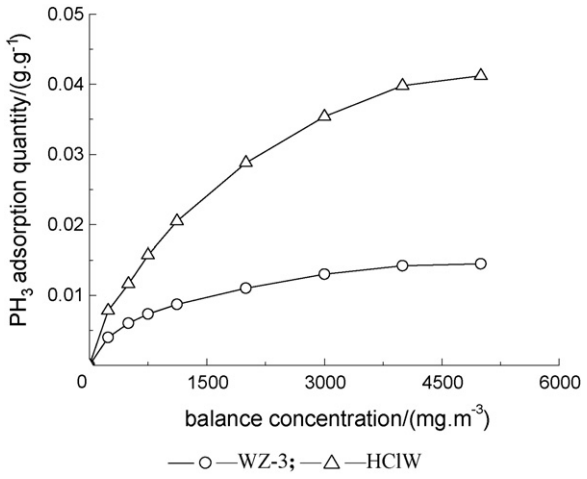

Fig. 4. Adsorption isotherms at 20 °C and 0.5% of O_2.

3. Results and discussions

3.1. Adsorbent screening

3.1.1. Effects of the types of adsorbents

The experiment studied four types of adsorbents with carriers: zeolite (ZMS-5A), ordinary activated carbon (AC) WZ-1, WZ-2, and WZ-3. Zeolite and activated carbon were continuously mixed with distilled water for 6 h at 70 °C to remove the soluble impurity in the adsorbents and then dried for 12 h at 110 °C [7]. Table 1 lists the physical performance parameters of the adsorbents.

Fig. 2 shows the adsorbent breakthrough curves of different types of adsorbents for PH_3. The results indicate that the adsorbent performance of ordinary activated carbon for PH_3 is always better than zeolite. Under the experimental conditions of 20 °C and 0.5% of oxygen, the adsorbent capacities were WZ-3 (0.0101, g/g) > WZ-2 (0.0084, g/g) > WZ-1 (0.0073, g/g) > zeolite (0.0036, g/g).

3.1.2. The effects of the types of modifiers on the adsorption for PH_3

The experiment harnessed impregnation to modify the activated carbon (WZ-3) and involved a solution of 7% hexanediol, KNO_3, or HCl. The solid was kept at 20 °C while three types of breakthrough curves for modifying the activated carbon were measured (Fig. 3) in order to test the different types of impregnates in their abilities to remove PH_3 at low concentrations through activated carbon. Fig. 3 shows that the adsorbent effects were greatly improved after being impregnated by HCl. The effects of hexanediol and KNO_3 used as dephosphorylation flux at lower temperatures were not obvious. The adsorbent capacity of activated carbon was three times as large as that of virgin activated carbon after being impregnated by 7% HCl.

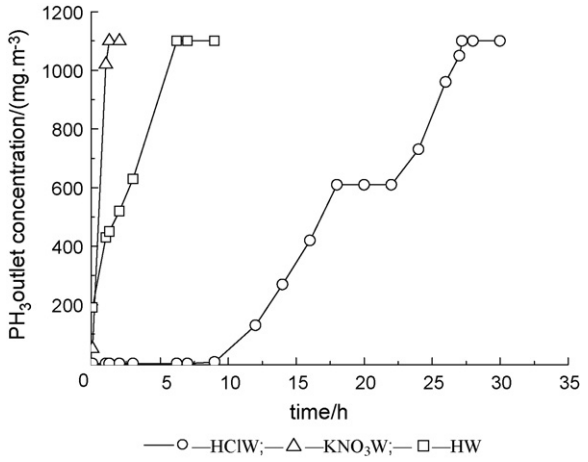

Fig. 3. Breakthrough curves of PH_3 on differently modified activated carbon at 20 °C and 0.5% of O_2 (PH_3 inlet concentration 1100 mg/m^3).

3.2. PH_3 adsorption isotherms

The PH_3 breakthrough curves on WZ-3 and HClW were drawn based on the points where the exit concentrations were 99% of the entrance concentrations (C/Co = 99%) of 250, 750, 1000, 2000, 3000, 4000, 5000 mg/m^3 at 20 °C according to type (1) calculation of adsorption capacities. The adsorption isotherms of PH_3 were determined based on the adsorption capacities. Fig. 4 shows the adsorption isotherms of PH_3 on WZ-3 and HClW. The activated carbon loaded with HCl had high activeness to PH_3, and the balance adsorption capacity increased significantly under the experimental conditions of 20 °C in temperature and 0.5% of oxygen. Within the concentrations tested, PH_3 adsorption isotherms on activated carbon and impregnated activated carbon were calculated according to Freundlich adsorption equation. The correlation stationary (R^2) was bigger than 0.99. Freundlich adsorption equations for adsorption of PH_3 on WZ-3 carbon and HClW-impregnated activated carbon were obtained at 20 °C after fitting as following:

$$q_e = 0.000417c_e^{0.4262} \quad (2)$$

$$q_e = 0.000351c_e^{0.5713} \quad (3)$$

In the equation: q_e = balance adsorption capacity, g/g; c_e = balance concentration, mg/m^3.

3.3. Effects of operating condition

3.3.1. Effects of reaction temperature

PH_3 breakthroughs in an HClW bed at 20 °C, 70 °C, and 110 °C were indicated in Fig. 5. The HClW sample in this experiment was produced by WZ-3-activated carbon that was modified in HCl. Reaction temperature was one of the most important factors that influenced purification efficiency in the process of impregnating activated carbon to purify PH_3. Fig. 5 shows that the efficiency of dephosphorization (the increasing of phosphorus capacity) was enhanced significantly by increasing the reaction temperature. Fig. 6 shows that, for HClW, the outlet concentration of PH_3 was below 1 mg/m^3 during the prior period before the breakthrough point when the temperatures higher than 70 °C. That is, the out-

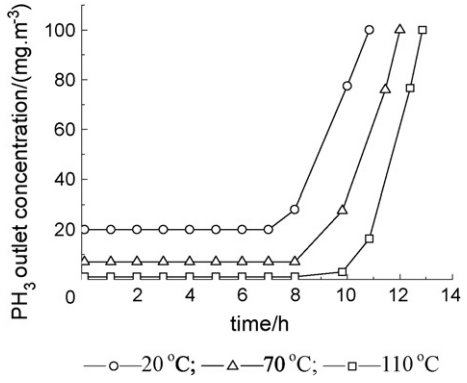

Fig. 5. Effects of reaction temperature on breakthroughs of PH_3 in a HClW fixed bed (O_2 at 0.1%, PH_3 inlet concentration 1100 mg/m^3).

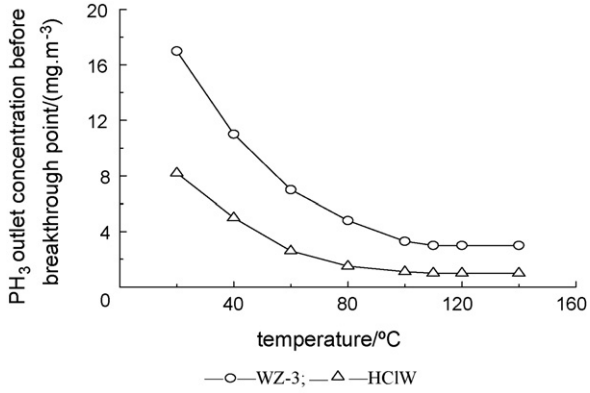

Fig. 6. Effects of temperature on PH_3 breakthrough point concentration in WZ-3 and HClW fixed beds (O_2 at 0.1%, PH_3 inlet concentration 1100 mg/m^3).

let concentration was below 1 mg/m^3 before breakthrough curve raise it's head. But when the temperature climbed up to a certain point (110 °C), the effects on purification efficiency for PH_3 were no longer obvious even if the temperature continued to climb. The "breakthrough point" was determined by PH_3 during the period when there was over 95% PH_3 removal efficiency. That is, the breakthrough point of the adsorbent was set at PH_3 outlet concentration of 55 mg/m^3.

3.3.2. Effects of oxygen content

Fig. 7 shows the oxygen content on PH_3 breakthroughs in HClW samples at 70 °C and at oxygen contents of 0.1%, 0.5%, 1.0%, and 1.5%, respectively [8]. Fig. 8 shows that the outlet concentration of PH_3 in HClW samples with different oxygen content conditions. Based on the data in Figs. 7 and 8, oxygen content was one of the most important factors that influenced impregnated activated carbon to purify PH_3 and the purification efficiency of PH_3 would be enhanced significantly by increasing the oxygen content. The increases in purification efficiency were not obvious when the oxygen content was higher than 1%. Fig. 8 also indicated that when the oxygen content was higher than 0.5%, the PH_3 content in the purified gas could meet the requirements of raw gas used to synthesize C1 chemical products (PH_3 < 1 mg/m^3).

3.4. Effects on pore size distribution

Fig. 9 shows the change of pore size distribution of HCl-modified activated carbon. Comparisons between WZ-3-activated carbon and HClW-modified activated carbon suggests that HCl modification resulted in a decrease in the volume of pores smaller than 2 nm

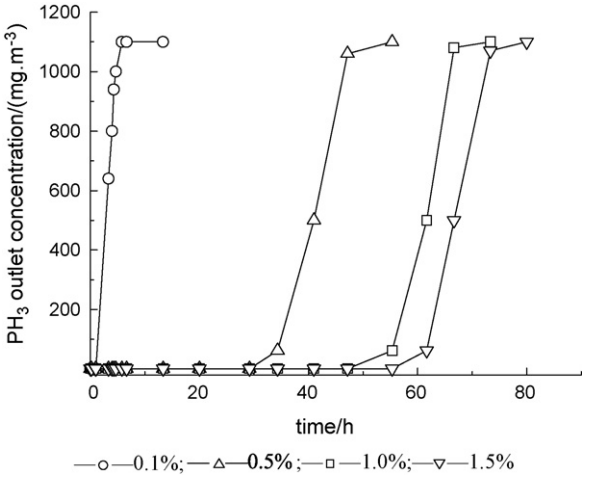

Fig. 7. Effects of oxygen content on PH_3 breakthrough in HClW bed at 70 °C (PH_3 inlet concentration 1100 mg/m^3).

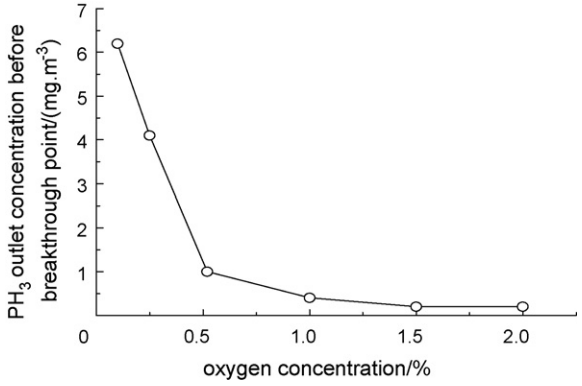

Fig. 8. Influence of oxygen content on breakthrough point concentration of PH_3 in a HClW bed at 70 °C (PH_3 inlet concentration 1100 mg/m^3).

and the most noticeable change was in the micropore volume of pores with sizes ranging from 0.3 nm to 1.5 nm. The results illustrated that HCl loaded in the sorbent was an effective component.

The comparison of HClW samples before and after adsorption showed that obvious differences only occurred in the micropore volume of pores with the size ranging from 0.3 nm to 1.5 nm. Obviously, the process in which PH_3 was oxidized into phosphorus oxide

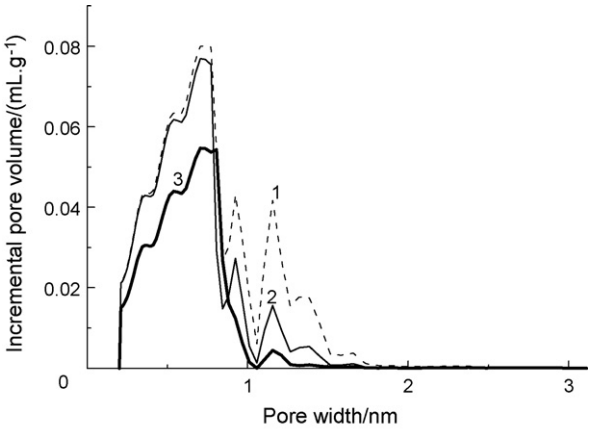

Fig. 9. Comparison of pore size distributions of HCl-modified samples before and after PH_3 adsorption.

Table 2
Structural parameters calculated from adsorption of impregnated carbons.

Samples	Specific surface area ($m^2\,g^{-1}$)	Micropore volume ($mL\,g^{-1}$)	Total pore volume ($mL\,g^{-1}$)	Average pore radius (nm)
WZ-3	1188	0.4980	0.5676	0.955
HClW	988	0.3842	0.4374	0.885
HClWE	716	0.2717	0.3105	0.867

(P_4O_{10} and H_3PO_4) occurred on these micropores [9,10]. If the catalytic oxidation reaction of PH_3 and HCl was the main adsorption process [11,12], the range of variations in micropore size could show that activated PH_3 was strongly adsorbed in the micropores after PH_3 was oxidized into phosphorus oxide.

Structural parameters of impregnated activated carbon after modification and adsorption are shown in Table 2. A comparison of WZ-3 and HClW samples showed that impregnation resulted in a decrease in the volume of pores smaller than 2 nm and accounted for 87% decrease in the total volume of pores. The surface areas decreased 17% and the volume decreased 23% in micropores with HCl modification. The pore distribution indicated that all micropores were influenced by the impregnation process.

Fig. 9 and Table 2 show the comparison between HClW samples and HClWE samples. HClWE is the spent adsorbent. PH_3 adsorption caused significant changes in sorbent voidage. The surface areas decreased 28%, 29% of which was due to the decrease in micropore volumes after modification. Thus, the activated carbon micropore activity in the PH_3 oxidation process can be inferred—HCl loaded in the micropores played a catalytic role in PH_3 oxidation and adsorption.

3.5. X-ray photoelectron spectroscopic (XPS) analysis

In order to analyze the mechanism of HCl-activated carbon, which is an oxidation adsorption reaction on the surface, it is necessary to analyze the reaction products and the DTA curves around the adsorption [13].

The chemical states of the elements on the HClWE adsorbent (after adsorption) were examined by XPS. Fig. 10 shows the XPS spectra of core level binding energy in P2p after adsorption/oxidation. The XPS fitting data of the P peaks, the possible P statuses, and their relative percentages are summarized in Table 3.

As shown by Fig. 10 and Table 3, the P2p peak centered at 133.62 eV indicates the possible presence of H_3PO_4 and the P2p peak centered at 135.07 eV indicates the possible presence of $P_4O_{10}(P_2O_5)$. The H_3PO_4 and P_4O_{10} species appeared in the HClWE sample were generated by an oxidation process. Freshly prepared HClW adsorbent had no P species. After adsorption, it was observed that the relative percentage of H_3PO_4 (59.77%) was more than that of P_4O_{10} (40.23%) [14].

The above findings indicated that HCl played a very important role in the reaction process in which the activated carbon adsorbed PH_3 and the process in which HCl was fixed on the surface of activated carbon. There was no doubt that H_3PO_4 and P_4O_{10} were formed in much higher quantity than on the carbon sample without HCl. The data suggest that HCl may play a role in catalytic oxidation during the process in which the activated carbon adsorbed PH_3.

Table 3
XPS data of the P2p spectra and their possible P statuses after PH_3 adsorption.

P status	Before adsorption HClW	After adsorption HClWE	
	P2p	H_3PO_4	P_4O_{10}
Binding energy of P2p (eV)	–	133.62	135.07
fwhm (eV)	–	2.06	2.03
Calculated P percentage (%)	0	59.77	40.23

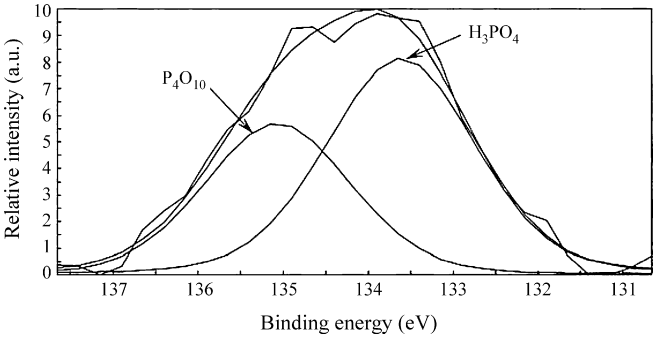

Fig. 10. XPS spectra of HClWE for P2p.

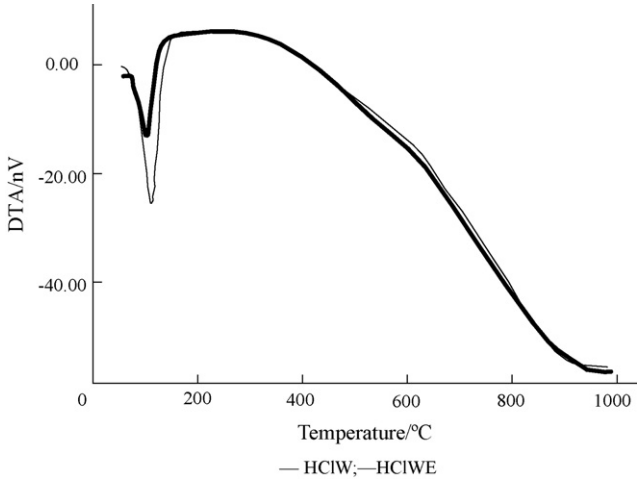

Fig. 11. DTA curves in nitrogen for the initial and exhausted carbon impregnated with HCl.

3.6. Analyses of thermo-gravimetry and heat athermalization

Fig. 11 shows the differences between HClW and HClWE in DTA curves. Only one clear heat adsorption peak was observed around 100 °C in DTA curves, but the weightlessness and the heat absorption intensity of HClW samples increased significantly after the adsorption. HClWE showed a heat adsorption peak whose intensity was much greater than that from HClW in DTA curves. Its shape was due to water loss [6]. HClWE heat adsorption peak was much greater than that from HClW, indicating that H_2O was generated or activated carbon adsorbed H_2O during the adsorption process.

On the other hand, H_3PO_4 decomposition temperature is 300 °C, P_4O_{10} sublimation temperature is 347 °C. P_2O_3 boiling point temperature is 175 °C. So Fig. 10 indicates that the adsorbed substance did not include P_2O_3 since the sample heat adsorption peak was not at 175 °C.

4. Conclusions

Activated carbon that was modified by impregnation, especially by HCl impregnation, could significantly enhance the adsorption purification ability. A sorbent modified by 7% HCl (mass fraction) was applied in the adsorption purification of PH_3 and 0.041 g/g was the adsorption capacity. The outlet break-point concentration of PH_3 was less than 1 mg/m^3, which could meet the standard of

off-gas to be used as the raw material gas to produce C1 chemical products after purification.

Two key factors that impacted the purification process were discovered: one was the reaction temperature in the process of using modified activated carbon to adsorb and purify PH_3 and the other was the oxygen content in the gas. Raising the reaction temperature or increasing the oxygen content of the gas can improve the purification efficiency significantly.

The reduction in the adsorbent's total pore volume after modification mainly occurred in pores below 2 nm in diameter, especially in the range of 0.3–1.5 nm. The pore volume decreased significantly after modification and the decrease in micropore volume accounted for 87% of the total volume change. After adsorption, the surface areas decreased 28%, 29% of which was due to micropore surface decrease. HCl significantly increased the performance of carbon as a PH_3 adsorbent when HCl impregnation was applied whereas the effects of other materials used in this study were much less pronounced. As a result of this process, oxidation products were strongly adsorbed and present in small pores ranging from 0.3 nm to 1.5 nm. It was likely that HCl present in the micropores acted as a catalyst for oxygen activation causing PH_3 oxidation into H_3PO_4 and P_4O_{10}. In conclusion, this study shows that impregnated activated carbon can be used in further purification of low concentration phosphine.

Acknowledgements

This study was funded by "863"National High-tech Development Plan Foundation (No. 2004AA649040) and by The National Natural Science Foundation of China (No. 50708044).

References

[1] P. Ning, X.Q. Wang, M.C. Wu, L. Chen, Y.H. Chen, K.C. Pan, Y. Wu, Purifying yellow phosphorus tail gas by caustic washing catalytic oxidation, Chem. Eng. (China) 10 (2004) 61–65.
[2] M.C. Wu, P. Ning, B.N. Ren, X.Q. Wang, The progress of purifying yellow phosphorus tail gas, Inorg. Chem. Ind. 9 (2003) 1–3.
[3] P. Ning, Y.C. Xie, H.H. Yi, Study on a four-bed PSA process for the manufacture of pure CO, in: Proceedings of the Seventh International Conference of Fundamentals of Adsorption, Nagasaki, Japan, 2001, pp. 613–617.
[4] Z.D. Ren, L. Chen, P. Ning, Y.H. Chen, K.C. Pan, H.J. Zhang, Research on technology of purifying yellow phosphorus tail gas to produce formic acid and dimethyl carbonate, Chem. Eng. (China) 34 (2006) 62–65.
[5] L.V. Gonchamva, S.K. Clowes, R.R. Fogg, et al., Phosphine adsorption and the production of phosphide phases on Cu (0 0 1), Surf. Sci. 515 (2002) 553–566.
[6] J.B. Teresa, Effect of pore structure and surface chemistry of virgin activated carbons on removal of hydrogen sulfide, Carbon 37 (1999) 483–491.
[7] B. Andrey, J.B. Teresa, H_2S adsorption/oxidation on unmodified activated carbons: importance of prehumidification, Carbon 39 (2001) 2303–2311.
[8] J.B. Teresa, On the adsorption/oxidation of hydrogen sulfide on activated carbons at ambient temperatures, J. Colloid Interface Sci. 246 (2002) 1–20.
[9] B. Svetlana, S.B. Frederick, W. Xianxian, et al., Activated carbon catalyst for selective oxidation of hydrogensulphide: on the influence of pore structure, surface characteristics, and catalytically-active nitrogen, Carbon 45 (2007) 1354–1363.
[10] Y. Yegiazarov, J. Clark, L. Potapova, et al., Adsorption-catalytic process for carbon disulfide removal from air, Catal. Today 102–103 (2005) 242–247.
[11] C.C. Huang, C.H. Chen, S.M. Chu, Effect of moisture on H_2S adsorption by copper impregnated activated carbon, J. Hazard. Mater. 136 (2006) 866–873.
[12] N.T. Danh, J.B. Teresa, Activated carbons with metal containing bentonite binders as adsorbents of hydrogen sulfide, Carbon 43 (2005) 359–367.
[13] M.P. Cal, B.W. Strickle, A.A. Lizzio, High temperature hydrogen sulfide adsorption on activated carbon I. Effects of gas composition and metal addition, Carbon 38 (2000) 1757–1765.
[14] W.C. Li, H. Bai, J.N. Hsu, Metal loaded zeolite adsorbents for phosphine removal, Ind. Eng. Chem. Res. 47 (5) (2008) 1501–1505.